JOURNAL OF SOLID STATE CHEMISTRY 120, 54–59 (1995)

Possible Mechanisms for Applications of Polarizable and OH-Containing Glasses to MOS Devices

Keiji Kobayashi

Toshiba ULSI Research Center, 1-Komukai Toshibacho, Kawasaki, Japan

Received March 13, 1995; in revised form June 16, 1995; accepted June 20, 1995

The selection of materials for semiconductor device passivation was investigated as regards the application of ZnO- and PbO-based glasses in MOS (metal, oxide, and silicon) devices. It was found that mechanisms affecting the application of these glasses to MOS devices were related to the molar polarizabilities and the OH radical contents in glasses. With regard to the recovery of C–V (capacitance–voltage) hysteresis loops in MOS capacitors, ZnO-based glasses were found to be superior to PbO-based glasses, since the molar polarizability of ZnO-based glasses was smaller than that of PbO-based glasses. The concentration of OH radicals depends on the composition of the glasses and had a negative effect on the recovery of C–V curve shifts in MOS capacitors passivated by these glasses. The glasses had low-temperature reflow below 800°C; PbO-based glasses had lower flow points than ZnO-based glasses. The possible mechanisms for the recovery of $\Delta\overline{V}_G$ shifts in C–V hysteresis loops were elucidated by the use of Poisson's equation and OH absorption coefficients. © 1995 Academic Press, Inc.

1. INTRODUCTION

Dielectric glass films are an essential component of ULSI (ultra large-scale integration) devices, where they are used as interlayer insulators and multilevel interconnection insulators (1–3). Recently, there has been a particular need for low-temperature reflow glasses in highly integrated ULSI chips, since such chips require the formation of shallow junctions (4, 5). Highly doped and low polarizable borophosphosilicate glasses (BPSG) formed from inorganic sources by chemical vapor deposition have been adopted in some highly integrated ULSIs (6), but there is a tendency for BPO_4 crystallites to form (7). The precipitation of BPO_4 crystallites inhibits glass reflow, so this is a fatal drawback in terms of device planarization and the formation of multilevel interconnections (8). The results of many studies of inorganic BPSG have demonstrated that it is difficult to obtain homogeneous glasses without crystallites when the reflow temperature is below 800°C (7).

ZnO- and PbO-based glasses without crystallites have flow temperatures far lower than that of BPSG, but both are somewhat polarizable and contain a small quantity of OH radicals (9, 10). The concentration of OH radicals in ULSI insulator glasses can be obtained by measuring optical properties such as transmittance, absorption, and reflectivity. The introduction of fluoride ions with low polarizability and weak chemical bonds into glasses causes the removal of OH radicals (11) and improves the C–V (capacitance–voltage) characteristics in passivated MOS capacitors; fluoride-containing ZnO- and PbO-based glasses are particularly favorable for the formation of homogeneous films for use in device passivations, since they readily reduce the flow temperature. This paper deals with the optical, thermomechanical, polarizable, and MOS properties of low-temperature reflow and low OH-containing ZnO- and PbO-based device planarization glasses.

2. EXPERIMENTAL

Batches of ZnO–ZnF_2–SiO_2–B_2O_3–P_2O_5 and PbO–PbF_2–SiO_2–B_2O_3–Al_2O_3 glasses were prepared from reagent grade chemicals. The ZnO-based glasses were melted at 1300°C for 5 h and PbO-based glasses were melted at 1200°C for 5 h. Melting was carried out in a platinum crucible using an electric furnace under an oxidizing atmosphere. After they were melted, the glasses were poured onto a stainless steel plate and then annealed. Infrared spectra were measured using a Digi-Labo spectrophotometer with 10 × 20 × 1 mm plates. Thermal expansion curves were measured using Rigaku TMA systems. Glass transition points and flow points were determined using thermal expansion curves obtained on 20-mm-long, 4.5-mm-diameter rods.

The molar polarizability of the glass was calculated, as previously described by the author (10, 12). Sputter target glasses were cut and ground to 75.0-mm-diameter, 10-mm-thick shapes. Glass films 2000 Å thick were sputtered on a SiO_2 layer (500 Å) formed on Si(100) wafers at 1 kW power and 30 m Torr using a Perkin–Elmer vacuum system. Glass thickness was measured by the

0022-4596/95 $12.00
Copyright © 1995 by Academic Press, Inc.
All rights of reproduction in any form reserved.

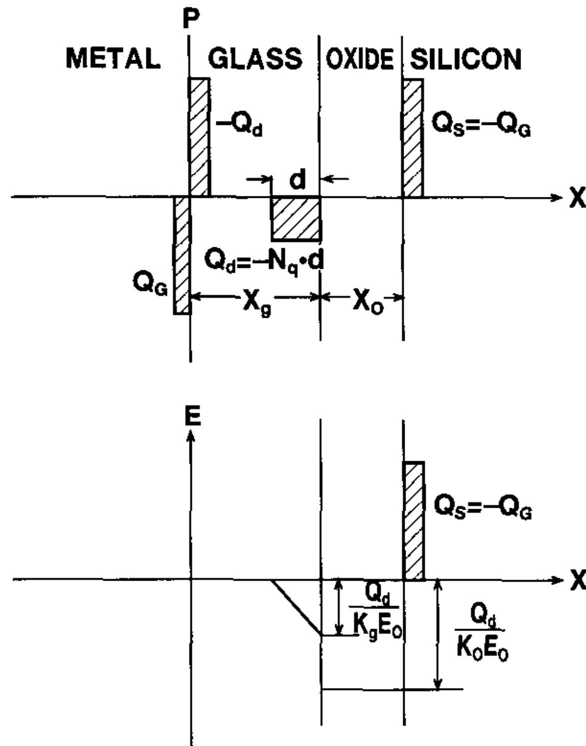

FIG. 1. Charge distribution and electric field in MOS capacitors.

use of a Nanometrics SD9-2000T thickness-meter using the Na–D-line refractive index (N_D = 1.56). Aluminum electrodes were deposited on the glass film. C–V curves for the MOS capacitors were observed at 1 GHz at room temperature.

3. DISCUSSION AND RESULTS

3.1. *Theory of MOS Capacitors Passivated by Glasses*

The potential for application of glasses in ULSI device passivation can be demonstrated by measuring the C–V characteristics of MOS capacitors passivated with the glasses. The C–V curve shifts toward higher voltage as the molar polarizability of the glass increases. This adverse effect on the C–V curve has been described in terms of the polarizing voltage, V_p, in MGOS (metal, glass, oxide, and silicon) structure (13, 14), in which Poisson's equation is written as

$$-V_p = (N_q d^2/2K_g E_0) + N_q d X_o/K_o E_0, \qquad [1]$$

where d is the charge width, representing the charge distribution in the glass, N_q is the polarizable ion concentration at charge q, Q_s is the surface charge accumulated on the silicon surface, X_g and X_o are the glass and oxide film thicknesses, respectively, and K_g and K_o are the glass and oxide dielectric constants, respectively. E_0 is the dielectric permittivity of free space. The charge distribution in the glass and the electric field in the MOS capacitor are shown in Fig. 1. Solving Eq. [1] for d results in

$$d = \left(\frac{K_g^2 X_o^2}{K_o^2} - \frac{2E_0 K_g}{N_q} \cdot V_p\right)^{1/2} - \frac{K_g X_o}{K_o}. \qquad [2]$$

When the glass molar polarizability is very small, $V_p \simeq 0$ and, therefore, $(2E_0K_g/N_q)V_p \simeq 0$. If this term $(2E_0K_g/N_q) \cdot V_p$ is then neglected in Eq. [2], $d \simeq 0$ is obtained. Therefore, in Fig. 1, Q_d and Q_s (= Q_d/K_oE_0) become very small.

TABLE 1
ZnO- and PbO-Based Glass Compositions, T_{OH}, R_{OH}, β_{OH}, $\Delta\overline{V}_G$, and T_f

Glass no.	ZnO	ZnF_2	B_2O_3	SiO_2	Al_2O_3	P_2O_5	P_m	T_{OH} (%)	R_{OH}	β_{OH} (cm^{-1})	$\Delta\overline{V}_G$ (V)	T_f (°C)
1	52	1	36	6	2	3	0.395	23	0.52	2.0	1.0	595
2	54	1	31	6	3	5	0.410	21	0.54	2.1	2.5	590
3	54	1	33	4	3	5	0.409	17	0.58	2.4	3.0	587
4	54	1	34	2	3	6	0.408	3	0.83	3.8	3.6	580
5	55	1	30	2	3	9	0.414	2	0.86	4.0	4.5	570

Glass no.	PbO	PbF_2	SiO_2	B_2O_3	Al_2O_3	P_m	T_{OH} (%)	R_{OH}	β_{OH} (cm^{-1})	$\Delta\overline{V}_G$ (V)	T_f (°C)
6	19.0	0.5	56.0	20.0	4.5	0.359	9.0	0.70	3.08	5.5	570
7	22.0	0.5	52.0	21.0	4.5	0.402	8.0	0.72	3.18	5.5	560
8	31.0	0.5	40.0	25.0	3.5	0.531	23.0	0.52	2.01	4.8	540
9	49.0	0.5	13.5	37.0	0	0.786	42.0	0.35	1.06	4.0	520
10	54.0	0.5	14.5	31.0	0	0.864	46.0	0.32	0.91	3.5	505

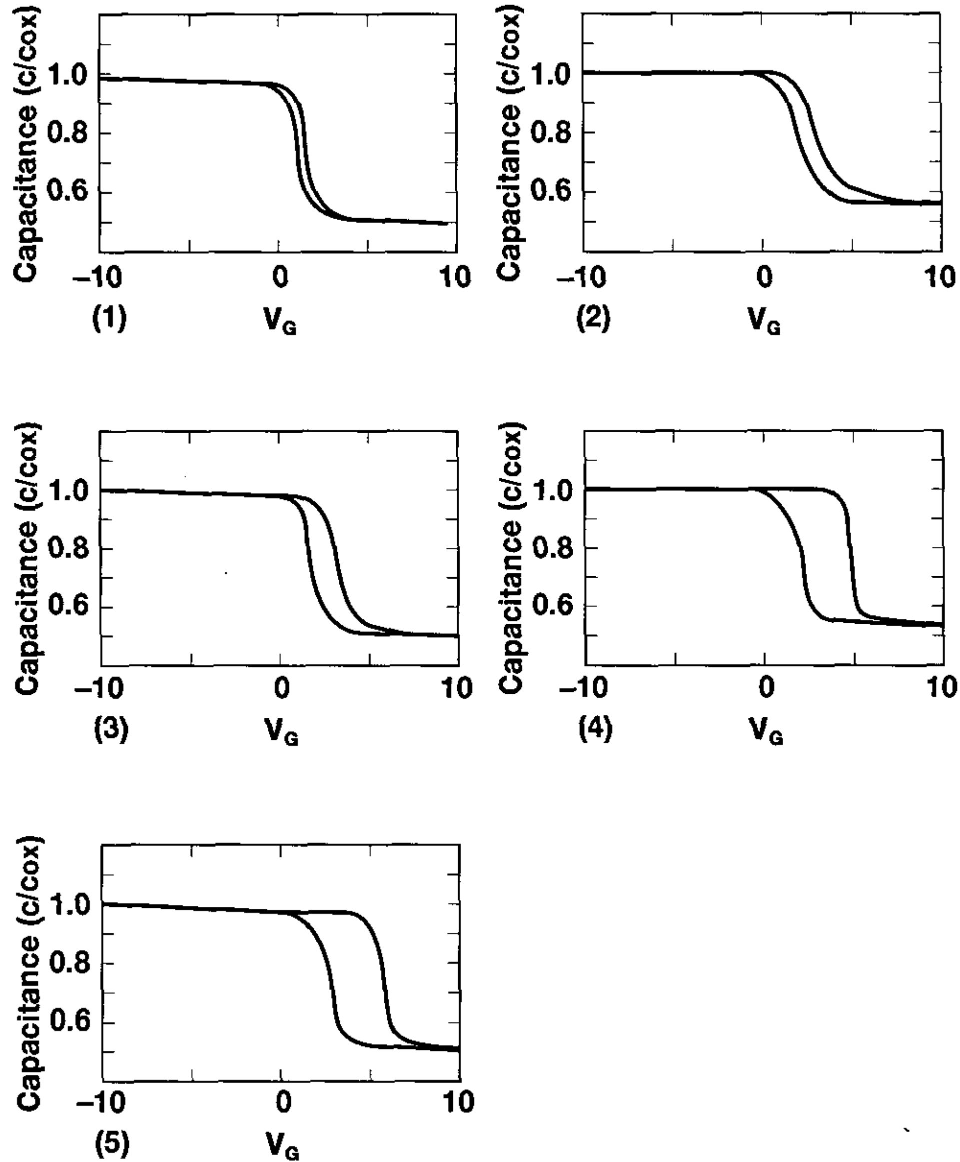

FIG. 2. C–V hysteresis loops for rapid thermal annealed MOS capacitors passivated by ZnO- and PbO-based glasses. Plates (1)–(10) represent passivation by the respective glass numbers.

Snow and Dumesnil (13) deduced the relationship between the C–V curve shift, $\Delta\overline{V}_G$, and Q_s, as given by

$$\Delta\overline{V}_G = Q_s/C_o, \quad [3]$$

where C_o is the oxide film capacitance. Since Q_s and Q_d depend on glass polarizability, so does $\Delta\overline{V}_G$ in Eq. [3].

Molar polarizability P_m can be described as

$$P_m = \sum P_i m_i \quad [4]$$

where P_i is the molar polarizability and m_i is the composition making up the glass (mole%). Polarizable mobile ions are introduced at the metal–oxide interface and transported through the oxide to accumulate near the semiconductor electrode. The induced charge causes the C–V characteristics of the device to shift toward the right. This charge storage adversely affects MOS device electric properties (13).

3.2 Polarizable, Optical, Thermomechanical, and MOS Properties of Glasses

The compositions of ZnO- and PbO-based glasses prepared in this work are given in Table 1, along with various

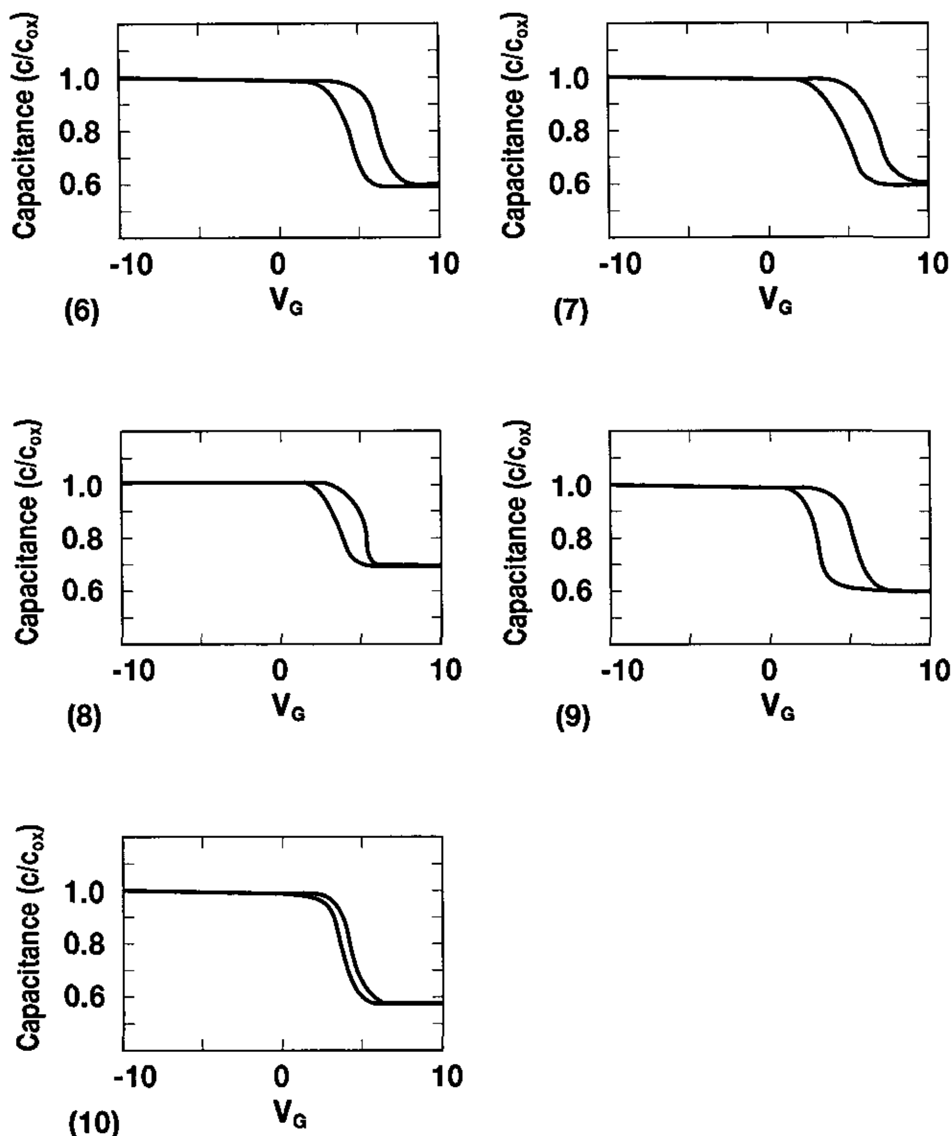

FIG. 2—*Continued*

characteristics. Glass transition points, $T_g(\log \eta = 13.3)$, flow points, $T_f(\log \eta = 10)$, thermal expansion coefficients, α, OH absorption coefficients β_{OH}, transmittances around OH band, T_{OH}, reflectivities around OH band, R_{OH}, molar polarizabilities, P_m, and C–V curve shifts, $\Delta\overline{V}_G$, are listed in Table 1. $\Delta\overline{V}_G$ is the mean value at the midpoints of the front and back of the hysteresis curves. The molar polarizabilities, P_m, for the ZnO- and PbO-based glasses are calculated from the equations

$$P_m = 0.72m_{Zn^{2+}} + 0.0076m_{B^{3+}} + 0.084m_{Si^{4+}} + 0.136_{Al^{3+}} + 0.054m_{P^{5+}} \quad [5]$$

$$P_m = 1.56m_{Pb^{2+}} + 0.084m_{Si^{4+}} + 0.0076m_{B^{3+}} + 0.136m_{Al^{3+}}, \quad [6]$$

where the constants of molar polarizabilities are obtained from Vleck's data (15).

C–V curves for MOS capacitors passivated by ZnO-based and PbO-based glasses are shown in Fig. 2, plates (1)–(10). The composition of the glass after sputtering deviated somewhat from the bulk composition. The content of ZnO in films showed a decrease of 3% and the content of PbO in films showed a decrease of 5%, in comparison with the compositions of the bulk glasses. The

other oxides such as SiO_2, B_2O_3, P_2O_5, and Al_2O_3 in films were the same composition as the bulks.

It is reasonable to suppose that these peculiar C–V curve shifts and the hysteresis loops are affected by the polarizing voltage and the OH absorption in the glasses (16–18). Both effects have been shown to give rise to the hysteresis curve feature and $\overline{V}_G$ shift toward the higher voltage. The OH content probably arises from a glass batch composition containing water and the OH ions react with fluoride ions, as represented by

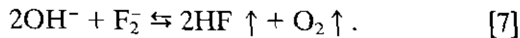

$$2OH^- + F_2^- \leftrightarrows 2HF \uparrow + O_2 \uparrow . \quad [7]$$

It is presumed that the reversible reaction in a pyrohydrolysis phenomena controls the OH concentration in glasses. Infrared OH absorption spectra for ZnO- and PbO-based bulk glasses 1 mm thick are given in Fig. 3 plates (1)–(10).

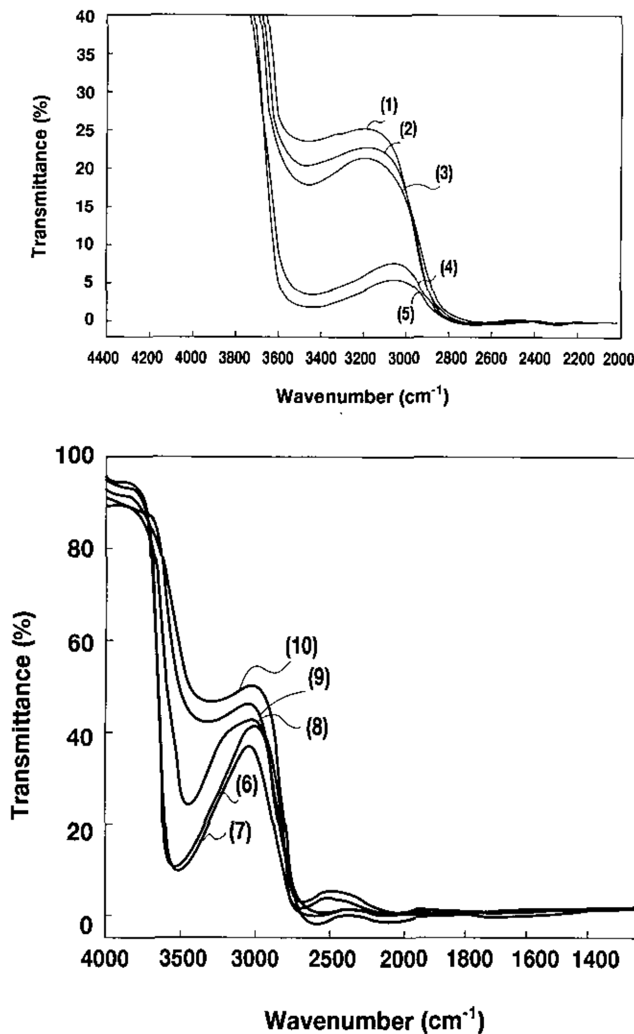

FIG. 3. Infrared absorption spectra for ZnO- and PbO-based glasses. Plates (1)–(10) represent the respective glass numbers.

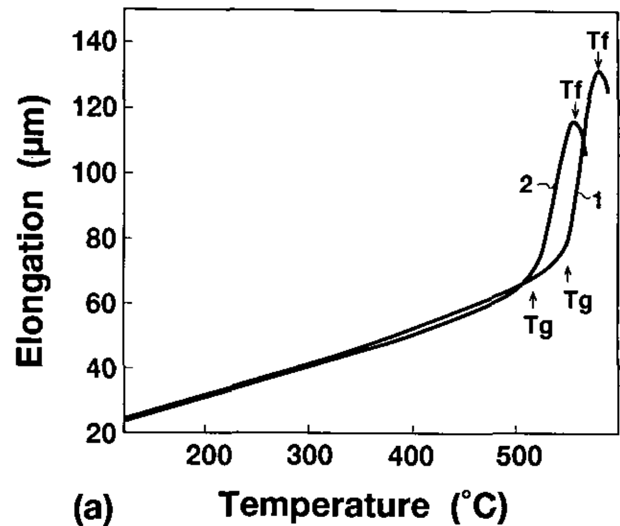

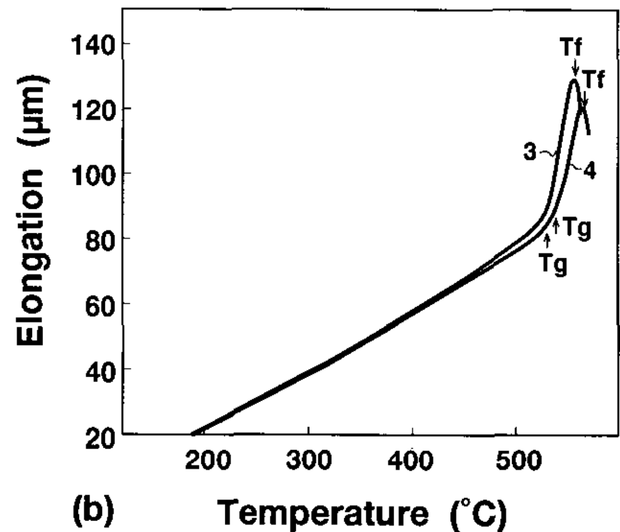

FIG. 4. Typical thermal expansion curves for ZnO- and PbO-based glasses. 1, glass No. (1); 2, glass No. (5); 3, glass No. (6); and 4, glass No. (7).

Impurities in the OH absorption bands around 3500 cm^{-1} varied with the composition of the glasses. The relationships between T_{OH} and R_{OH} can be represented as (19)

$$T_{OH} = 1 - [R_{OH}(1 - R_{OH}) + R_{OH}] = (1 - R_{OH})^2. \quad [8]$$

The absorption coefficient, β_{OH}, resulting from the fundamental vibration of OH radicals at around 3500 cm^{-1} is calculated from (20)

$$T_{OH} = [(1 - R_{OH})^2 e^{-\beta_{OH} t}]/[1 - R_{OH}^2 e^{-2\beta_{OH} t}], \quad [9]$$

where t is the glass thickness.

By substituting Eq. [8] into Eq. [9], Eq. [9] can be simplified to

$$1 = e^{-\beta_{OH} t} + R_{OH}^2 e^{-2\beta_{OH} t} \qquad [10]$$

The OH absorption coefficients, β_{OH}, are computed from Eq. [10], using a microcomputer.

Optical values of T_{OH}, R_{OH}, and β_{OH} calculated from the infrared absorption spectra are also listed in Table 1. The author has focused on two factors for the deformation and the shift of the hysteresis *C–V* curves, namely the effects of polarizability and OH radicals in glasses.

Typical thermal expansion curves for ZnO- and PbO-based glasses are given in Figs. 4a and 4b, respectively. Assuming that these glasses will be used as semiconductor insulators, low-temperature reflow below 800°C has been studied in an effort to obtain highly doped borophosphosilicate glasses. These ZnO- and PbO-based glasses showed far lower flow points than those for borophosphosilicate glasses reported previously. In particular, flow points for PbO-based glasses were lower than those for ZnO-based glasses. The flow temperature was determined by Baret *et al.* (21), using the thermal expansion curves.

4. CONCLUSIONS

The recovery of $\Delta\overline{V}_G$ shifts depends on both the molar polarizability and OH radical content. This recovery is more pronounced in ZnO-based glasses than in PbO-based glasses, since ZnO-based glasses have lower polarizability than PbO-based glasses. The concentration of OH radicals indicates that the total oxide charge increases. This positive oxide charge derives from hydrogen-related vacancies (16). The loss of hydrogeneous species is related to the disappearance of hysteresis in the *C–V* curve (16). A hydrogeneous complex is responsible for the carrier trapping mechanism (16). MOS capacitors passivated by ZnO-based glasses with a minimum content of OH radicals and low polarizability showed the best recovery of *C–V* characteristics and flowed at below 800°C. The possible mechanisms for the $\Delta\overline{V}_G$ shift in MOS capacitors was discussed in terms of Poisson's equation in MOS capacitors using values of β_{OH} calculated from infrared absorption spectra.

REFERENCES

1. S. Itoh, Y. Homma, and E. Sasaki, *J. Vac. Sci. Technol. A* **9,** 2696 (1991).
2. T. Homma and Y. Murao, *J. Electrochem. Soc.* **140,** 2046 (1993).
3. S. Itoh *et al., J. Electrochem. Soc.* **137,** 1212 (1990).
4. S. Sze, *in* "Proceedings, 14th International Conference on Solid State Devices, Tokyo, Japan, 1982"; *Jpn. J. Appl. Phys. (Suppl.)*, 3 (1982).
5. L. Zambov *et al., Solid-State Electron.* **34,** 1239 (1991).
6. S. Rojas *et al., J. Vac. Sci. Technol. B* **10,** 633 (1992).
7. G. L. Schnable, A. W. Fisher, and J. M. Shaw, *J. Electrochem. Soc.* **137,** 3973 (1990).
8. K. Kobayashi, *J. Mater. Sci. Lett.* **13,** 1446 (1994).
9. K. Kobayashi, *J. Mater. Sci. Lett.* **13,** 1764 (1994).
10. K. Kobayashi, *J. Non-Cryst. Solids* **124,** 229 (1990).
11. K. Kobayashi, *J. Electrochem. Soc.* **131,** 2190 (1984).
12. K. Kobayashi, *J. Non-Cryst. Solids* **109,** 277 (1989).
13. E. H. Snow and M. E. Dumesnil, *J. Appl. Phys.* **37,** 2123 (1966).
14. K. Kobayashi, *Appl. Phys. Lett.* **51,** 1600 (1987).
15. V. Vleck, "Theory of Electric and Magnetic Susceptibilities" (Translated into Japanese by M. Kotani), p. 241. Yoshioka, Tokyo, 1958.
16. S. C. Li *et al., J. Appl. Phys.* **72,** 2947 (1992).
17. A. K. Bandyopadhyai *et al., J. Mater. Sci. Lett.* **8,** 1464 (1989).
18. M. A. Villegas *et al., J. Mater. Sci.* **23,** 2464 (1988).
19. J. A. Ruller and J. E. Shelby, *Phys. Chem. Glasses* **33,** 177 (1992).
20. L. Zhenhua and G. H. Frischat, *J. Non-Cryst. Solids* **163,** 169 (1993).
21. G. Baret, R. Madar, and C. Bernard, *J. Electrochem. Soc.* **138,** 2836 (1991).